Supplementary Materials and Methods

1. Production process flow for yeast protein powder based on *Saccharomyces cerevisiae* ZAB 02 (CGMCC No. 27288)

The process mainly includes the following core steps: strain activation and expansion, fermentation culture, cell harvest and disruption, protein extraction and drying.

Step 1: Strain activation and seed expansion. Strain revival: The original strain ZAB 02 is retrieved from the preservation tube and inoculated under sterile conditions onto agar plates containing YPD solid medium. It is then incubated at a constant temperature of 28-30 °C for 48-72 hours to revive the dormant strain. Preparation of primary seed culture: Single colonies are selected and inoculated into sterile YPD liquid medium in Erlenmeyer flasks, then cultivated on a shaking incubator at a speed of 150-200 rpm and 30° C for 18-24 hours to obtain an activated seed culture. Secondary Expansion: The primary seed culture is transferred to a larger seed tank containing a greater volume of culture medium at a specific inoculation ratio for scaling up. This step is aimed at obtaining a sufficient quantity of uniform physiological state cells, preparing for large-scale fermentation inoculation. Secondary expansion: The primary seed culture is transferred to a larger seed tank containing a greater volume of culture medium at a specific inoculation ratio (e.g., 1-5% v/v) for scaling up. This step is aimed at obtaining a sufficient quantity of uniform physiological state cells, preparing for large-scale fermentation inoculation.

Step 2: Large-scale fermentation culture. Inoculation of fermentation tank: The

high-density secondary seed culture is pumped into a sterilized large fermentation tank according to an optimized inoculation ratio. The fermentation tank is filled with an optimized medium, typically containing molasses or glucose as the carbon source, and ammonia, urea, or ammonium sulfate as nitrogen sources, along with necessary inorganic salts and growth factors. Nutrient feeding: Continuous or batch feeding techniques are employed to supply concentrated nutrients (primarily carbon sources), avoiding substrate inhibition and prolonging the exponential growth phase of the cells, thereby significantly increasing cell density and total protein yield. End of fermentation assessment: When the residual sugar in the fermentation broth drops to a certain level, and the cell density no longer shows significant increases, the fermentation is deemed complete. Typically, the fermentation cycle lasts 15-20 hours.

Step 3: Cell harvesting and disruption. Centrifugal separation: Upon completion of fermentation, high-speed tubular or disk centrifuges are used to separate the yeast biomass from the culture medium, resulting in wet yeast paste. Washing: The wet yeast paste is washed with purified water or buffer solution to remove residual culture medium components and metabolic wastes. Cell Disruption: Yeast cells possess a robust cell wall that must be disrupted to effectively release the intracellular proteins.

Step 4: Protein extraction and product processing. Separation and concentration: The disrupted slurry undergoes solid-liquid separation (e.g., further centrifugation or filtration) to remove cell wall debris, resulting in a protein-rich extract. Drying: The yeast protein extract is dried using a spray dryer, where the liquid material is atomized into fine droplets and instantly evaporated when in contact with hot air, forming a

powder product that is easy to store and transport. Packaging and quality control: The dried yeast protein powder is cooled and sieved under sterile conditions for standardized packaging. Finally, strict quality inspection of the finished product is conducted, including assessments of protein content, moisture, ash content, and microbial indicators, to ensure compliance with established standards.

Table S1 Yeast protein (SGS Sample ID: QDF23-040327.001) composition table

Composition	Content (g/100 g)
Aspartic acid	8.62
Threonine	4.35
Serine	4.21
Glutamic acid	10.39
Gluycine	3.53
Alanine	4.81
Valine	5.26
Isoleucine	4.76
Leucine	7.22
Tyrosine	3.57
Phenylalanine	4.34
Lysine	7.55
Histidine	1.87
Arginine	4.93
Proline	3.21
Tryptophan	1.06
Cysteine	0.66
MetSON	1.54
Total of amino acid	81.88
Total fat	8.24
Saturated fat	1.68
Trans fat	0.08
Total (Fructose+Glucose+Sucrose+Maltose+Lactose)	0
Water	3.6
Ash	3.3
Nucleic acid	1.3

2. Dose conversion from humans to mice based on body surface area (BSA)

Based on recommendations from Zhen-Ao Group Co., Ltd. and the Science and Technology Development Center of the China Health Food Association, the suggested daily yeast protein intake for adults (average body weight 60 kg) is 6 g/day, equivalent to an average daily dietary intake of 100 mg/kg. Mouse body weight was recorded every 3 days. The daily yeast protein intake for mice was then calculated using the animal equivalent dose formula (Table S2). The calculation formula is as follows:

Daily yeast protein intake for mice (mg/kg) = [Adult daily yeast protein intake (100 mg/kg) × Adult body weight (60 kg) / Adult body surface area value (1.6246 m^2)] × [Mouse body surface area value (0.0076 m^2) / Mouse body weight (kg)].

Table S2 Commonly used data for dose conversion between different animal species [1]

Animal species	Meeh-Rubner K-value	Weight (kg)	Body Surface Area (m^2)	Mg/kg-mg/m^2 Transfer Factor	Relative surface area per kilogram of body weight
Mice	9.1	0.018	0.0066	2.9	1 (0.02kg)
		0.02	0.0067	3	
		0.022	0.0071	3.1	
		0.024	0.0076	3.2	
Human	10.6	40	1.2398	32.2	0.08 (50.0 kg)
		50	1.4386	34.8	
		60	1.6246	36.9	

Table S3 Daily oral and gavage doses of yeast protein in mice

Day	Yeast protein intake (mg)				
	CO	OB	OM	GB	GM
1	0	31.73	59.98	32.07	53.58
3	0	31.01	53.03	21.84	54.76
5	0	31.66	54.14	23.05	55.35
7	0	28.94	49.49	22.02	54.49
9	0	33.15	56.69	25.61	55.32
11	0	34.09	58.30	27.02	55.37
13	0	33.29	56.94	27.26	54.92

15	0	33.61	57.48	28.25	54.87
17	0	33.50	57.29	28.96	55.50
19	0	33.18	56.74	29.53	54.80
21	0	33.84	57.87	30.75	56.21
23	0	33.63	57.52	31.39	56.25
25	0	33.67	57.58	32.97	55.66
27	0	34.65	59.25	34.40	56.67
29	0	33.94	63.28	33.00	57.42

3. Selection criteria for mice sample size and sex

In this study, a sample size of eight mice per group was employed, which is common and justified in the field of nutritional intervention and aging phenotype research. This sample size effectively controls for inter-individual variability while providing a reliable data foundation for subsequent statistical analysis. It also aligns with the "3R principles" (Replacement, Reduction, and Refinement) of animal research ethics. This study aims to preliminarily investigate the effects of yeast protein on physiological functions (particularly the musculoskeletal system) and aging-related biomarkers, as well as its underlying mechanisms. The estrous cycle in female mice induces periodic fluctuations in physiological hormone levels, which may directly interfere with various observed indicators such as bone metabolism, inflammatory status, and gut microbiota. This could introduce considerable variation, potentially masking the specific effects of the intervention. In this initial mechanism-exploration stage, the use of a single gender (male) is a common strategy within the field. This approach aims to minimize the confounding effects of gender and hormonal cycles, thereby helping to more clearly reveal the causal relationship between the intervention and the core phenotypes, laying a foundation for more in-depth follow-up studies [2].

4. DNA extraction and 16S rRNA sequencing

Total microbial genomic DNA was isolated from mouse fecal samples using the FastPure Stool DNA Isolation Kit (MJYH, Shanghai, China). DNA quality and concentration were assessed by 1.0% agarose gel electrophoresis and a NanoDrop 2000 spectrophotometer (Thermo Scientific, United States), respectively, and samples were stored at –80 °C until further analysis. The V3–V4 hypervariable region of the bacterial 16S rRNA gene was amplified with the primer pair 338F (5′-ACTCCTACGGGAGGCAGCAG-3′) and 806R (5′-GGACTACHVGGGTWTCTAAT-3′) using a T100 Thermal Cycler (Bio-Rad, USA). Each 20 μL PCR reaction contained 4 μL of 5× Fast Pfu buffer, 2 μL of 2.5 mM dNTPs, 0.8 μL of each primer (5 μM), 0.4 μL Fast Pfu polymerase, and 10 ng template DNA, with ddH_2O added to volume. The PCR protocol comprised an initial denaturation at 95 °C for 3 min; 27 cycles of denaturation at 95 °C for 30 s, annealing at 55 °C for 30 s, and extension at 72 °C for 45 s; a final extension at 72 °C for 10 min; and a hold at 4 °C. Amplicons were excised from a 2% agarose gel, purified with the PCR Clean-Up Kit (YuHua, Shanghai, China) following the manufacturer's instructions, and quantified using a Qubit 4.0 fluorometer (Thermo Fisher Scientific, USA).

Purified amplicons were pooled in equimolar amounts and paired-end sequenced on an Illumina Nextseq2000 platform (Illumina, San Diego,USA) according to the standard protocols by Majorbio Bio-Pharm Technology Co. Ltd. (Shanghai, China).

After demultiplexing, the raw sequences were subjected to quality filtering using fastp (v0.19.6) and merged with FLASH (v1.2.11). High-quality sequences were then processed with the DADA2 plugin within the QIIME 2 pipeline (version 2020.2) using

recommended parameters to perform sample-specific error profile modeling and generate amplicon sequence variants (ASVs) at single-nucleotide resolution. To mitigate the influence of sequencing depth on diversity analyses, samples were rarefied to 20,000 sequences per sample, which maintained an average Good’s coverage of 97.90%. Taxonomic classification of ASVs was conducted using a Naïve Bayes classifier implemented in QIIME 2 against the SILVA 16S rRNA database (release 138). Functional potential of the microbial communities was predicted using PICRUSt2 (Phylogenetic Investigation of Communities by Reconstruction of Unobserved States) based on the ASV representative sequences. The PICRUSt2 workflow involved multiple steps: HMMER was employed for alignment of ASV sequences to reference databases; EPA-ng and Gappa were used for phylogenetic placement of sequences into a reference tree; Castor performed 16S gene copy number normalization; and MinPath generated metabolic pathway predictions from inferred gene families. The entire process followed the standard PICRUSt2 protocol.

Bioinformatic analysis of the gut microbiota was performed on the Majorbio Cloud Platform (https://cloud.majorbio.com). Based on the amplicon sequence variants (ASVs), rarefaction curves were generated and alpha diversity indices—including observed ASVs, Chao1 richness, Shannon index, and Good’s coverage—were calculated using Mothur (v1.30.1). Beta diversity was assessed by principal coordinate analysis (PCoA) based on Bray–Curtis dissimilarity with the Vegan package (v2.5-3) in R. To identify differentially abundant bacterial taxa across phylogenetic levels (from phylum to genus), community bar plots and Circos plots were employed. Ternary

diagrams were used to visualize the composition and distribution of dominant species among three sample groupings. Species exhibiting strong associations in Spearman correlation analysis were further selected for microbial co-occurrence network construction. Finally, ordinal regression analysis was applied to evaluate the relationships between individual clinical factors and microbial community structure, quantifying the contribution of each clinical variable to inter-sample compositional variation.

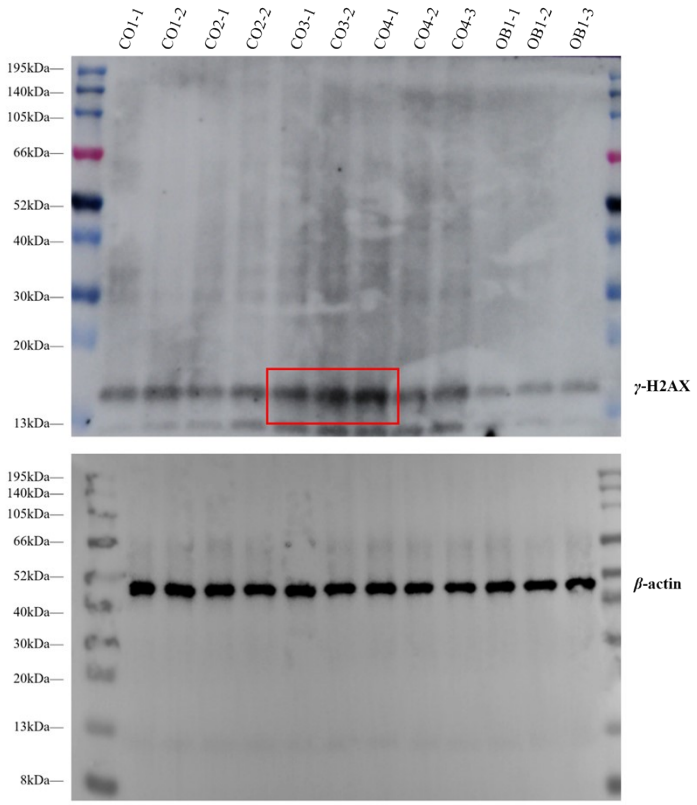
CO1-1
CO1-2
CO2-1
CO2-2
CO3-1
CO3-2
CO4-1
CO4-2
CO4-3
OB1-1
OB1-2
OB1-3
195kDa
140kDa
105kDa
66kDa
52kDa
40kDa
30kDa
20kDa
13kDa
γ-H2AX
195kDa
140kDa
105kDa
66kDa
52kDa
40kDa
30kDa
20kDa
13kDa
8kDa
β-actin

162

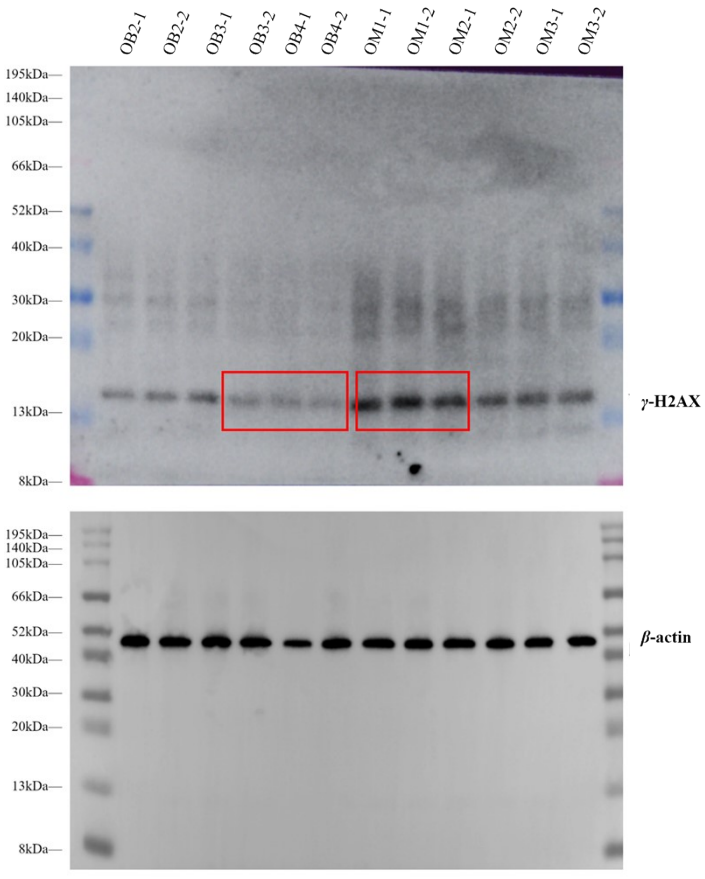
OB2-1
OB2-2
OB3-1
OB3-2
OB4-1
OB4-2
OM1-1
OM1-2
OM2-1
OM2-2
OM3-1
OM3-2
195kDa
140kDa
105kDa
66kDa
52kDa
40kDa
30kDa
20kDa
13kDa
8kDa
γ-H2AX
195kDa
140kDa
105kDa
66kDa
52kDa
40kDa
30kDa
20kDa
13kDa
8kDa
β-actin

163

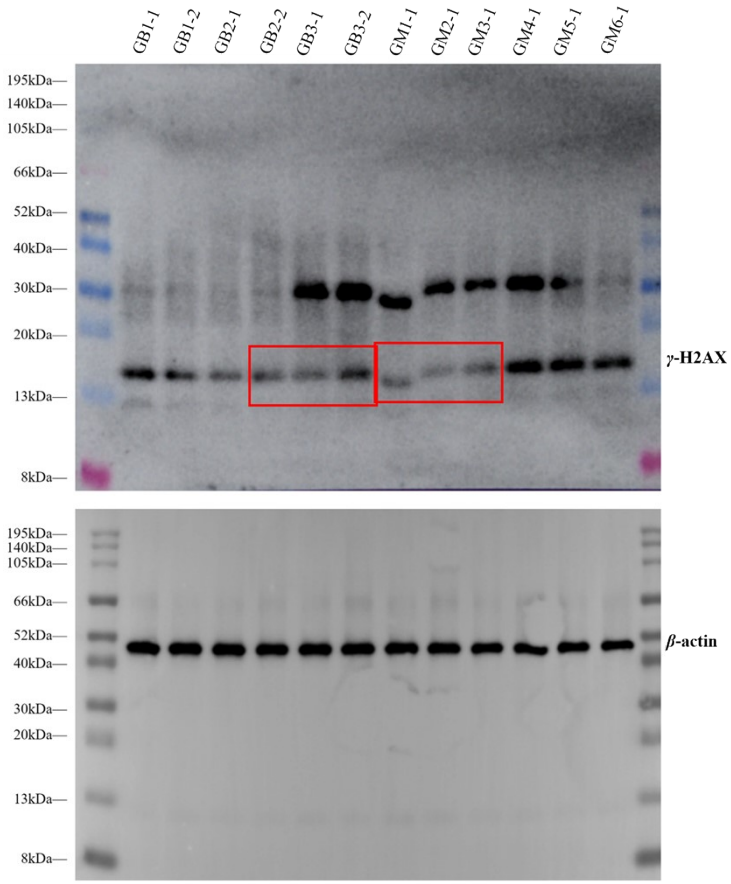

Figure S1. Western blot image showing *γ*-H2AX expression in the liver. The red box in the figure indicates the WB strip in Figure 4.

Reference

[1] Reagan-Shaw S, Nihal M, Ahmad N. Dose translation from animal to human studies revisited. Faseb j, 2008, 22(3), 659-661. DOI: 10.1096/fj.07-9574LSF.

[2] Best L, Dost T, Esser D, Flor S, et al. Metabolic modelling reveals the aging-associated decline of host-microbiome metabolic interactions in mice. Nat Microbiol. 2025 Apr;10(4):973-991. DOI: 10.1038/s41564-025-01959-z.F.